IET Microwaves, Antennas & Propagation

Research Article

IET Journals
The Institution of Engineering and Technology

Miniaturised printed elliptical nested fractal multiband antenna for energy harvesting applications

ISSN 1751-8725
Received on 6th November 2014
Revised on 29th January 2015
Accepted on 16th February 2015
doi: 10.1049/iet-map.2014.0744
www.ietdl.org

Mansour Taghadosi, Lutfi Albasha ✉, Nasser Qaddoumi, Mai Ali

Department of Electrical Engineering, American University of Sharjah, PO Box 26666, Sharjah, Dubai, UAE
✉ *E-mail: lalbasha@aus.edu*

Abstract: This study presents the design, optimisation, simulation and fabrication of a novel printed elliptical nested fractal (planar) antenna for multiband operation. The proposed antenna is intended to function as the receptor element in radio-frequency energy harvesting applications. The simple microstrip structure and the compact size of the antenna ease its fabrication and allow it to be integrated with other electronic circuitry. It consists of nested elliptical structures fed by 50 Ω microstrip line with complementary elliptical ground along with rectangular ground plane. The added Hilbert structures at both sides of the antenna feeding line on the top layer enhance its performance to operate in multi-frequency bands. This antenna exhibits good radiation and reflection characteristics at 910 MHz (global system of mobile (GSM 900)), 2.4 GHz (Bluetooth/wireless local area network), 3.2 GHz (Radiolocation, third generation (3G)), 3.8 GHz (for long-term evolution, 4G) and additional 5 GHz band (wireless fidelity signals). The overall dimension of antenna is 41 mm (width) × 44 mm (length) × 1.778 mm (thickness). To the best knowledge of the authors, this is the widest bandwidth antenna to be developed at these small dimensions covering major standards from 900 MHz up to 6 GHz for electromagnetic energy harvesting applications.

1 Introduction

Recently, multiband antennas have gained interest in radio-frequency (RF) energy harvesting applications. The multiband feature in such systems helps in scavenging ambient electromagnetic (EM) energy of the surrounding environment. EM energy is diverse in frequency and power. The power of the available signal for harvesting is too weak, so the antenna that will be used in these systems needs to have a high gain with an omni-directional pattern to harvest energy from different directions. Hence, an antenna with a single compact structure is required for such systems to perform the task of multiple antenna units. Apart from energy harvesting applications, multiband antenna is also widely used in wireless technologies where different sets of operating frequencies are desired such as in smart phones, multimedia devices etc. Multiband antenna reduces the size as well as the cost of the overall system functioning in a multi-standard system.

Several antennas for energy harvesting applications have been presented in the literature [1–4]. Antennas in harvesting circuits could operate using a single frequency, harvesting the power from single source of energy. For example, the harvesting system in [1] uses a planar circular spiral inductor antenna operating at 520 MHz. Functioning in a single frequency, this harvesting system is not capable of harvesting the abundant power available in other frequency bands. A dual-band planar antenna for RF energy harvesting was presented in [2]. This design utilises monopole antenna with three microstrip lines sharing the same feeding point. At this point, the overall impedance is matched at two frequency bands. Although those two bands are utilised in this antenna, the spectrum shows higher potentials by harvesting multiband frequencies. With the increasing demand for using renewable energy, the RF energy harvesting has improved recently. The demand for harvesting higher power requires these harvesting systems to operate at multi-frequencies. This helps such systems to harvest energy from the existing signals of different standards available in terms of different sources. The EM energy harvesting opportunities for 350–3 GHz spectrum has been studied in [3]. This paper indicates the higher power densities of global system of mobile (GSM 900), GSM 1800 and 2.4 GHz wireless fidelity (Wi-Fi) make them favourable for EM energy harvesting applications. In addition, in [3], the characteristics of single and dual-band textile antennas were predicted using numerical simulations. An EM energy harvesting using multiband planar antenna is presented in [4]. The proposed antenna in this paper resonates at different frequencies by creating different capacitances and inductances by altering the surface area of the meandered lines.

In this paper, the superiority of the miniaturised printed elliptical nested fractal (PENF) multiband antenna compared with all previous EM harvesting antennas presented in the literature lies in its wide multiband characteristics at different standard frequencies from 900 MHz up to 6 GHz. Furthermore, this novel microstrip fed antenna is simple, low weight and of compact size. The proposed antenna structure is fabricated using printed circuit board (PCB) technology and is easily connected to electronic circuitries (both surface mounted or integrated designs). This antenna does not require any vias or complicated geometries; hence, resulting in a very cost-effective structure.

Several multiband antennas have been presented in the literature in addition to harvesting applications [5–8]. A multiband printed dipole antenna is presented in [5]. The multiband response in this dipole antenna is achieved by adding reactive loads to the dipole antenna as metamaterial (MTM) inclusions. It has been shown that symmetrically loading the dipole antenna with a single MTM cell results in a dual-band response of the antenna. Furthermore, tri-band antenna was proposed by two loading approaches: the symmetrical loading is done by changing the location of the MTM cells and asymmetrical loading of the cells is done by loading the dipole antenna by two MTM cells having different gap widths. This antenna was optimised at both GSM 900 and GSM 1800 bands. In [6], a quad-band printed planar antenna fed by a 50 Ω microstrip line is presented. This antenna structure consists of three different U-shape stubs and L-shape monopole antennas which shows proper radiation in GSM 900, GSM 1800, 2.4 GHz Bluetooth/wireless local area network (WLAN) and 3.5 GHz worldwide interoperability for microwave access (WiMAX)

frequency bands. Despite the good performance of this antenna for mobile applications, it could not be used for applications where higher-frequency bands of operation are of interest. An asymmetric coplanar strip antenna functioning at three different frequency bands is presented in [7]. This inverted L-fed type antenna operates at 2.3, 3.5 and 5.3 GHz covering long-term evolution (LTE), WiMAX and IEEE802.11a standards, respectively. The antenna does not operate in the high-power GSM band that is useful for EM harvesting applications. The design of broad-side coupled antenna is presented in [8]. This antenna structure consists of a coupled loop with two branch lines and covers 694–960 MHz and 1710–2590 MHz frequency bands. This design does not cover high frequency bands and requires two shorting vias which snarls the fabrication process.

The selection of appropriate frequency bands is critical in RF energy harvesting applications. Scavenging RF signals from the portion of the spectrum with higher-power densities help in harvesting more energy from the ambience resulting in a more efficient harvester system. The selection of this portion of spectrum is certainly dependent on the existing signals of different standards available in the surrounding. On the basis of the citywide RF spectral surveys for EM energy harvesting conducted in [3, 9], the higher-power densities of existing ambient signals at GSM 900 (880–915 MHz, 925–960 MHz), GSM 1800 (1.71–1.785 GHz, 1.805–1.88 GHz), third generation (3G) (1.92–1.98 GHz, 2.11–2.17 GHz) and Bluetooth or Wi-Fi (2.4–2.468 GHz) direct the research of RF energy harvesting and its antenna design to target these specified frequency bands. Furthermore, the detailed power density measurements of GSM 900 and GSM 1800 presented in [10] affirm that despite of the wider bandwidth of the GSM 1800, the stronger narrow band peaks of GSM 900 are much more beneficial in terms of EM energy harvesting applications.

This paper presents the design, optimisation, simulation and fabrication of a novel PENF antenna for multiband operation. The proposed PENF antenna is intended to function as the receptor element in RF energy harvesting applications. This antenna exhibits a good radiation and reflection characteristics at 900 MHz (GSM), 2.4 GHz (Bluetooth/WLAN), 3.2 GHz (Radiolocation, 3G), 3.8 GHz (for LTE, 4G) and additional 5 GHz band (new Wi-Fi signals) and its overall dimension is very small (41 mm (width) × 44 mm (length) × 1.778 mm (thickness)).

The rest of this paper is organised as follows. The design of the proposed multiband antenna is described in Section 2. The characteristics of the antenna and simulation results using momentum three-dimensional (3D) planar EM simulator of advanced system design (ADS) are provided in Section 3. Moreover, fabrication and measurement results are provided in Section 4, whereas Section 5 includes the conclusions.

2 Antenna design and configuration

Planar antennas are created by etching different geometries on the conductor layers of PCB. The top conductor layer acts as the radiator or receptor element, whereas the bottom conductor layer acts as the ground plane [11]. These two layers are separated by the substrate insulation (dielectric) layer and the radiation occurs from the fringing fields between the edge of the created patch and the ground plane [12]. Planar antennas use different regular shapes to radiate EM waves. These printed monopole antennas could take a variety of geometries such as square, rectangular, hexagonal, triangular, circular and elliptical with different feed locations [13]. Among different shapes of patch antennas, elliptical antennas are of interest because of their circular polarisation. Printed elliptical antenna is an efficient radiator which offers a broadband feature which is of an interest in today's compact wireless systems [14, 15]. The design equations of printed elliptical monopole antenna are presented in [16]. The impedance matching technique provided in [16] indicates good performance of this type of antenna for high-bandwidth applications. This concept could be utilised further to have a multiband antenna covering different standards from 900 MHz up to 6 GHz by modifying the antenna's geometry.

The proposed PENF antenna structure is shown in Fig. 1. The antenna is fed by a 50 Ω microstrip line surrounded by three scaled-down repeated Hilbert fractal structures [17] to improve the impedance matching at multi-frequency bands. Larger scales of Hilbert fractal structures have been used to operate as multiband planar antennas because of their multi-resonance feature and compact size [18]. The main radiator (or receptor) element of the PENF antenna is the nested elliptical shapes which are commonly connected to the microstrip feed line. Each fractal elliptical structure along with its complementary ground elliptic shape on the bottom layer of PCB resonates at a certain frequency. Hence, this type of antenna architecture exhibits multiband response. The current design consists of four ellipses resulting in a major quad-band antenna. As an established fact, the inner ellipse is resonating at a higher frequency because of its smaller surface area, whereas the outer ellipse with larger surface area resonates at a lower frequency. The rest of the ellipses also play a part in determining the frequencies at which the antenna resonates. The ground layer, which is printed on the bottom of the substrate, consists of a rectangular ground plane positioned under the feed line and the Hilbert fractal structures in addition to the complementary nested elliptical shapes explained previously.

The proposed PENF antenna geometry was optimised to be fabricated on Rogers RT/Duroid 6010 laminate with a dielectric constant (ε_r) of 10.2, loss tangent ($\tan\delta$) of 0.0023, 70 mils (1.778 mm) thickness and 1 oz (35 μm) finished copper cladding

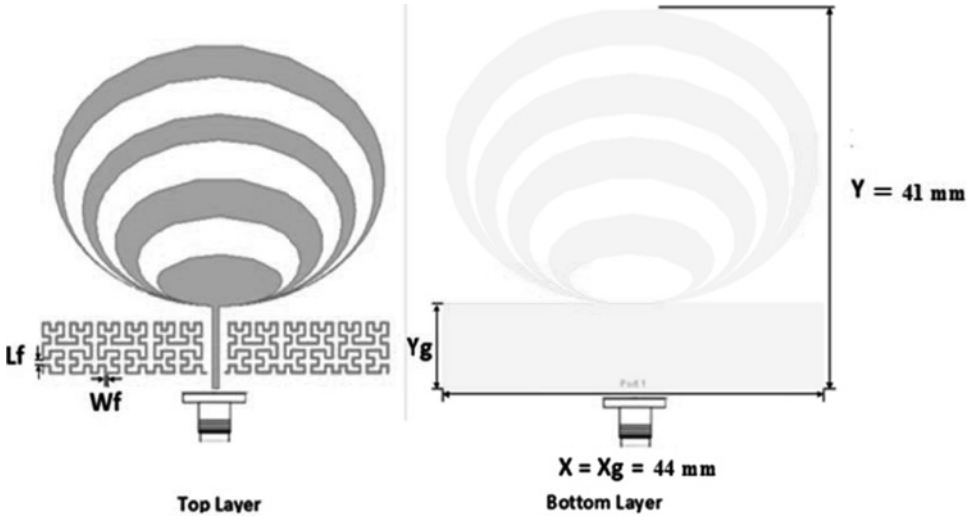

Fig. 1 *Geometry of the proposed PENF antenna*

IET Microw. Antennas Propag., 2015, Vol. 9, Iss. 10, pp. 1045–1053

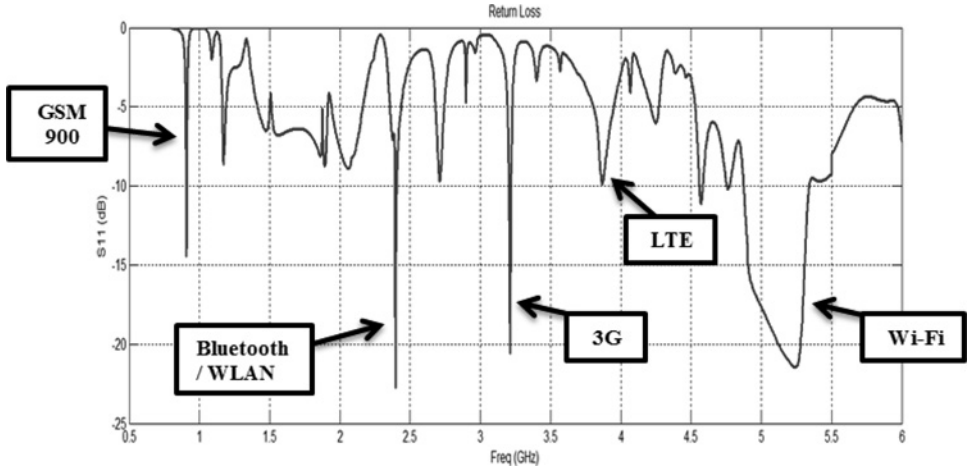

Fig. 2 *Simulated PENF antenna return loss response (70 mils Rogers 6010 substrate)*

(copper weight). The reason for selecting a high permittivity material is to achieve the required response by having more compact circuits and patches in the antenna, as the patch dimensions are inversely proportional to $\sqrt{\varepsilon_r}$ [19]. On the other hand, increasing the relative permittivity degrades the antenna performance in terms of the bandwidth and the radiation efficiency. Furthermore, the bandwidth and radiation efficiency of an antenna are proportional to the height of the substrate as well [20]. Hence, a thicker

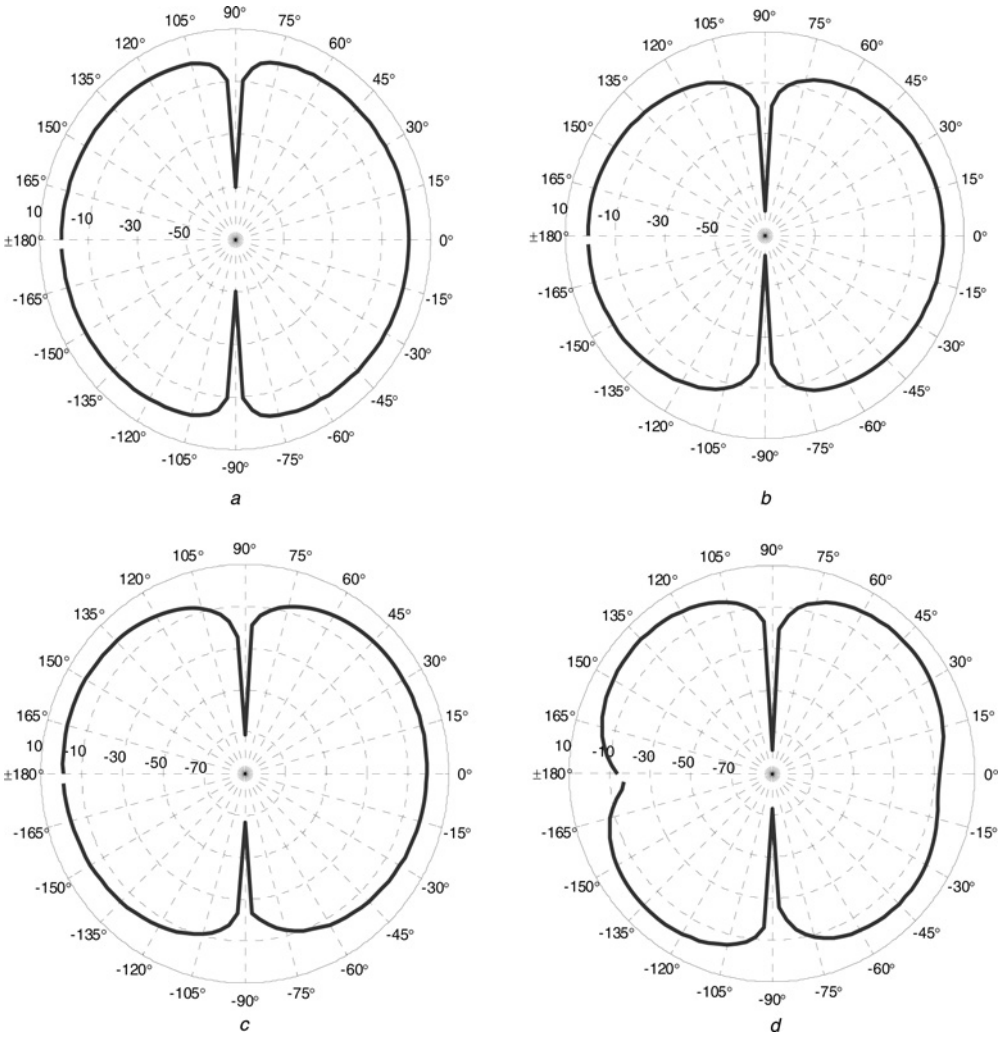

Fig. 3 *Simulated PENF antenna (Rogers 6010 substrate) gain at*

a 910 MHz
b 2.4 GHz
c 3.22 GHz
d 4.88 GHz

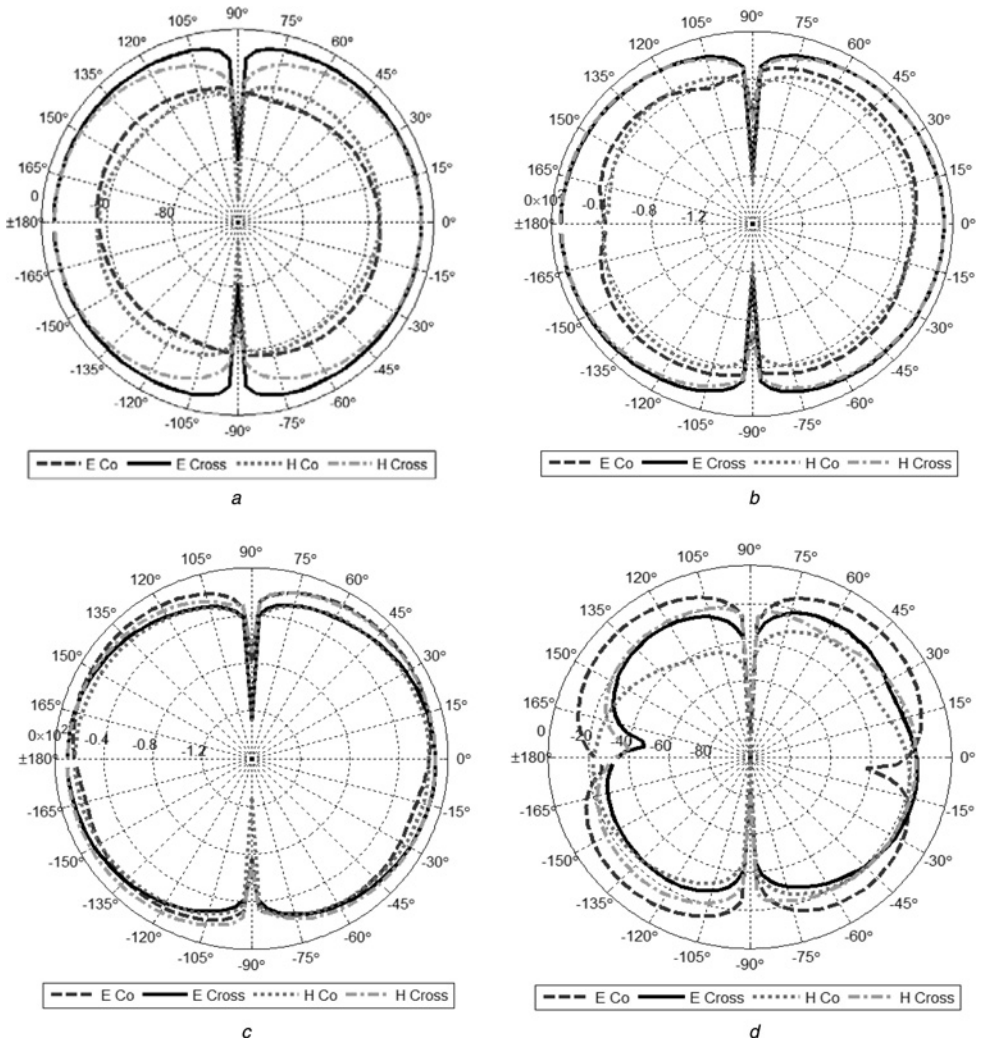

Fig. 4 *Simulated co-polarisation and cross-polarisation radiation patterns of PENF antenna (Rogers 6010 substrate) in E-plane and H-plane at*

a 910 MHz
b 2.4 GHz
c 3.22 GHz
d 4.88 GHz

substrate was selected to compensate for the larger permittivity considering the created surface waves which travel within the substrate and increase the side lobes. However, simulations and practical measurements of this research show that the PENF antenna also radiates at multiband frequencies when utilising different substrate materials with lower dielectric constants such as Flame Retardant 4 (FR4).

The width of the microstrip feed line of the antenna is 0.75 mm creating a 50 Ω line with a length of 9 mm. The rectangular patch in the ground layer has dimensions of 44×9 mm^2 (X_g and Y_g). The size of the overall antenna is optimised to be 44×41 mm^2 (X and Y). For this design, the fractal conductor width (w_f) is 0.18 mm and the length (L_f) is 0.6 mm. The optimum distances between the fractal geometry and the 50 Ω feed line of the PENF are 0.75 and 0.6 mm from the left and right, respectively.

3 Simulation results and discussion

Antennas are characterised by reflection and radiation properties. Reflection, which is the return loss characteristic, determines how well the antenna is capable of radiating or receiving power. It is a ratio of the reflected wave over the incident wave. In other words, it is a measure of impedance matching between the antenna and its feeding port (either source or load) at different frequencies. The radiation properties of an antenna display the direction (directivity), gain and the power density in which the antenna is radiating [21]. These parameters could be displayed as 2D or 3D graphs. To predict the response of the proposed PENF antenna, a simulation is performed using Momentum Simulator of ADS. The mesh frequency in the simulation setup is 10 GHz and the mesh density is specified to 30 cells per wavelength. This is a good and high-resolution setup for the interested frequency range of simulation.

Fig. 2 shows the return loss of the simulated antenna over the desired frequencies. As shown, the antenna exhibits a good return loss response at four major bands of 905–910 MHz (GSM 900),

Table 1 PENF antenna characteristics at different operating frequencies

Frequency, GHz	*S*11 magnitude, dB	Directivity, dBi	Gain, dBi	Input impedance, Ω
0.9075	−15	2.85	1.2	50 (0.74 − j0.21)
2.396	−21.2	4.7	1.63	50 (0.93 + j0.19)
3.219	−10.3	4.28	0.6	50 (1.14 + j0.67)
4.883	−11.4	6.5	1.24	50 (1.14 + j0.58)

IET Microw. Antennas Propag., 2015, Vol. 9, Iss. 10, pp. 1045–1053

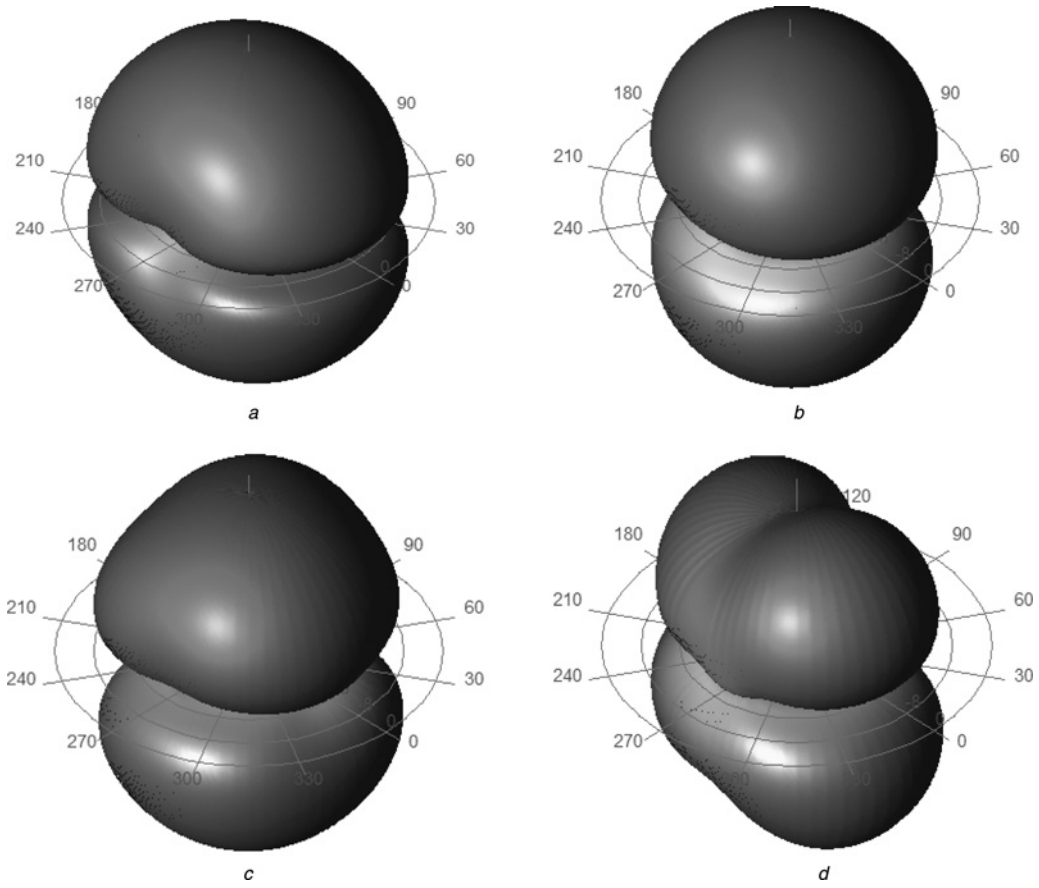

Fig. 5 *Simulated PENF antenna (Rogers 6010 substrate) 3D radiation pattern at*

a 910 MHz
b 2.4 GHz
c 3.22 GHz
d 4.88 GHz

Table 2 Comparison of the proposed PENF antenna against other antennas

References	Application	GSM 900	GSM 1800	Bluetooth/WLAN	**3G**	LTE/4G	Wi-Fi
[1]	EM harvester	no	no	no	no	no	no
[2]	EM harvester	yes	yes	no	no	no	no
[3]	EM harvester	yes	yes	no	no	no	no
[4]	EM harvester	no	yes	yes	no	no	yes
[5]	NA	yes	yes	no	no	no	no
[6]	mobile	yes	yes	yes	yes	no	no
[7]	mobile	no	no	yes	no	yes	yes
[8]	mobile	yes	yes	yes	no	no	no
PENF	EM harvester	yes	no	yes	yes	yes	yes

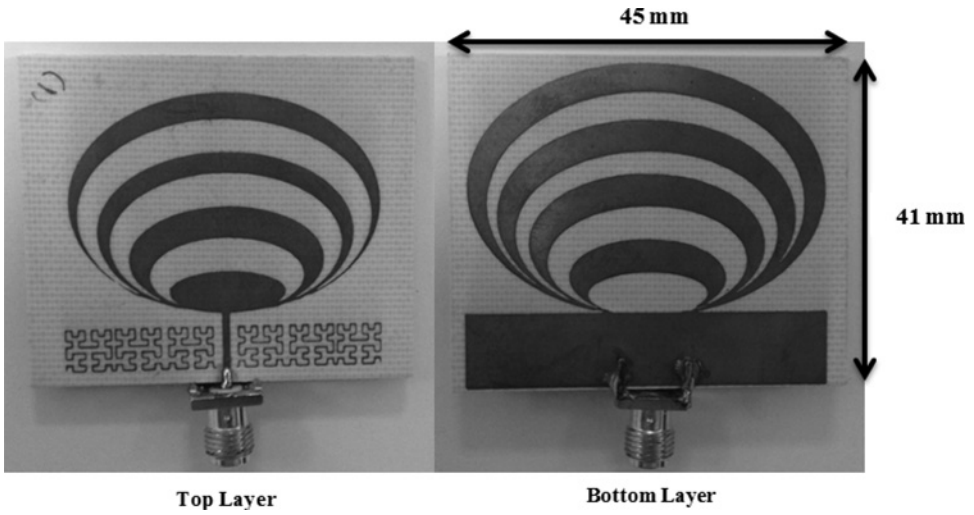

Fig. 6 *Fabricated PENF multiband antenna on FR4 substrate*

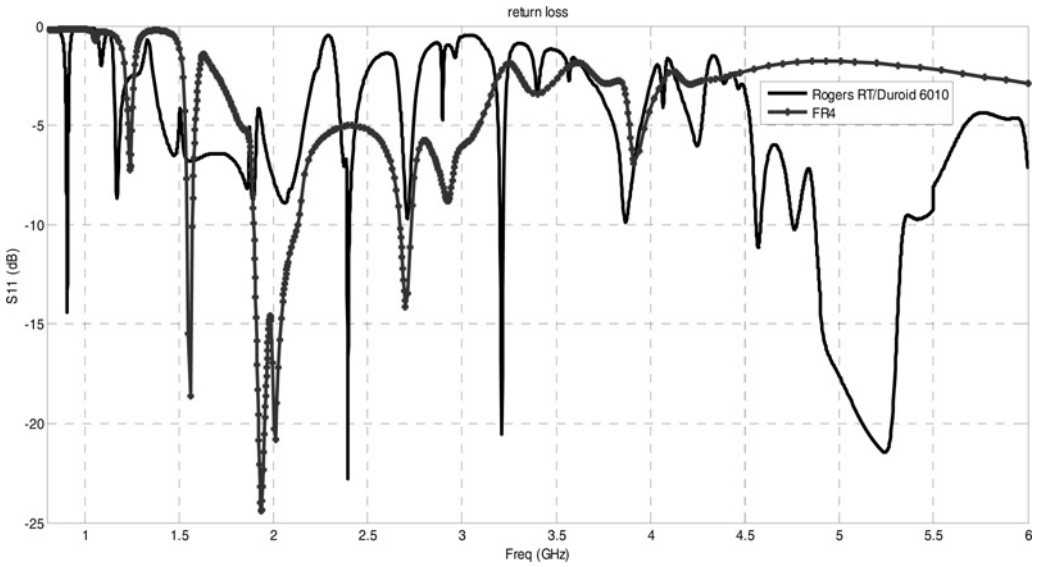

Fig. 7 *Simulated return loss response of PENF antenna designed on Rogers 6010 ($\varepsilon_r = 10.2$, $h = 1.778$ mm) substrate against FR4 ($\varepsilon_r = 4.55$, $h = 1.6$mm) substrate*

2.4 GHz (Bluetooth/WLAN), 3.2 GHz (3G) and 4.87–5.33 GHz (Wi-Fi). As seen in the figure, the return loss at these frequency bands is well below −10 dB ensuring proper impedance matching and reception of the antenna. In addition, the return loss is reasonable at other frequencies such as 2.7 GHz, 3.86 GHz (LTE) and 4.55–4.85 GHz, for which the return loss is close to −10 dB. Although the return loss is not optimal as in the major bands, it is helpful in harvesting energy from the available signals at this portion of the spectrum.

The simulated gain of the PENF antenna in a 2D plane is illustrated in Fig. 3. Moreover, Fig. 4 depicts the *E*-plane and *H*-plane cross- and co-polarisations. As shown in the figures, the radiation pattern of the antenna could be considered as omni-directional pattern. This type of radiation pattern is suitable for the EM energy harvesting applications where the direction of the available signal is unknown. Table 1 below presents a summary of the antenna characteristics at four major operating frequencies. As seen in this table, the antenna is showing a good return loss (better than −10 dB) at the listed frequencies; the simulated input impedance is fairly matched to 50 Ω. Moreover, the antenna offers acceptable directivity and gain values relative to an isotropic antenna.

Fig. 5 represents the simulated 3D radiation pattern of the PENF antenna for the frequency points listed in Table 1. As shown in the figure, for the first two frequencies, the radiation pattern is almost of a donut shape which indicates equal radiation in almost all directions (except at ±90°). As for the two higher frequencies, the antenna does not radiate equally in all directions.

Table 2 below presents a comparison between the PENF antennas against other antennas presented in the literature. The application as well as the operating standards of each antenna is indicated accordingly in the table.

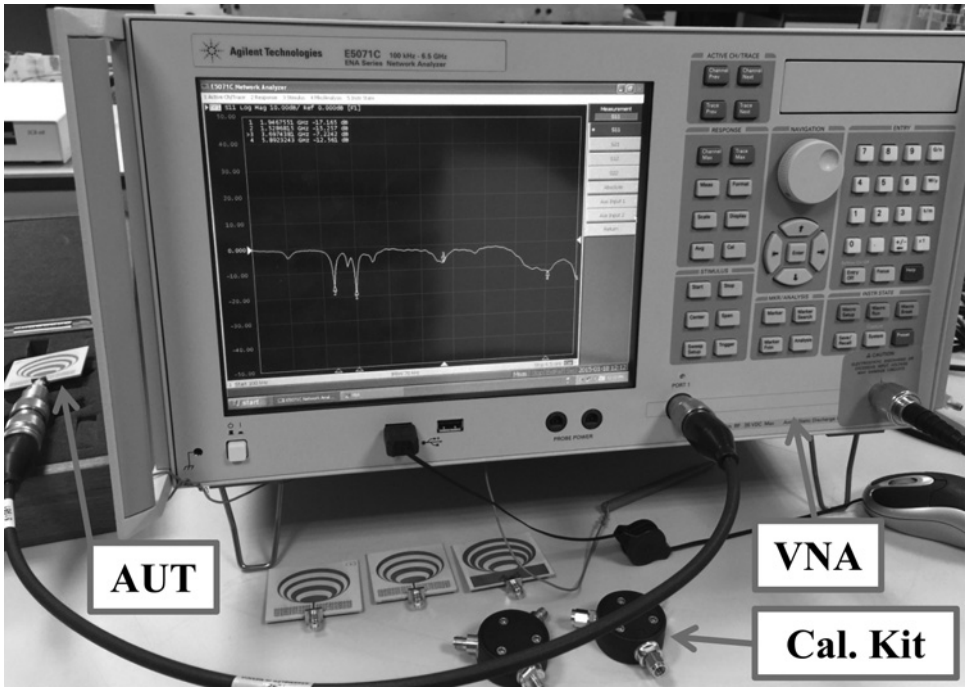

Fig. 8 *S11 measurement setup (AUT)*

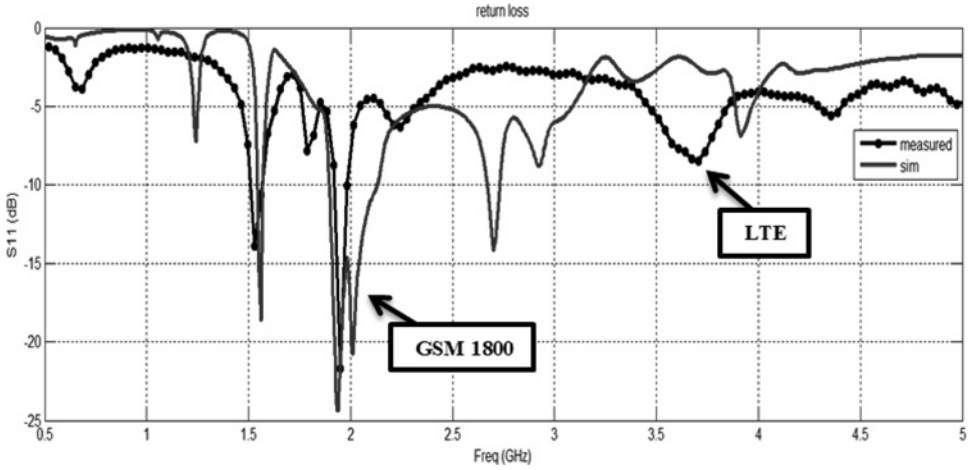

Fig. 9 *Comparison of the antenna's simulated return loss response in ADS (grey) against the partical measurent (black) is shown*

4 Antenna fabrication and measurement results

The PENF antenna was designed using Rogers 6010 RT/Duroid laminate. This laminate consists of two copper layers and an insulation layer in between. Hence, these laminates do not have any photoresist layer on the top of the conductor layers. The fabrication of Rogers laminates was not possible with the facilities available and the cost involved in fabricating overseas. Owing to this restriction, the PENF antenna was redesigned and fabricated using FR4 substrate (with a dielectric constant (ε_r) of 4.55, a loss tangent (tan δ) of 0.0175 and 1.6 mm thickness).

Fig. 6 shows the fabricated multiband antenna on FR4 substrate. During optimisation and simulation, the overall dimensions of the PENF antenna structure were kept the same as in the simulated Rogers substrate. Other dimensions of the antenna such as the ellipses, the Hilbert structure, the 50 Ω microstrip feed line and the ground plane were modified to compensate for the change in the permittivity of the newly used FR4 substrate. Although the optimisation of the PENF antenna was simulated using FR4 substrate, the optimum response at all desired standards was not achieved. Consequently, the size of the fabricated antenna is 4.5 × 4.1 cm^2. Fig. 7 presents the simulated return loss response comparison between the PENF antennas designed on Rogers 6010 ($\varepsilon_r = 10.2$, $h = 1.778$ mm) and FR4 ($\varepsilon_r = 4.55$, $h = 1.6$ mm) substrates.

In Fig. 8, the practical measurement setup is shown. The measurement setup consists of Agilent E5071C vector network analyser (VNA) and an antenna under test (AUT). Before the

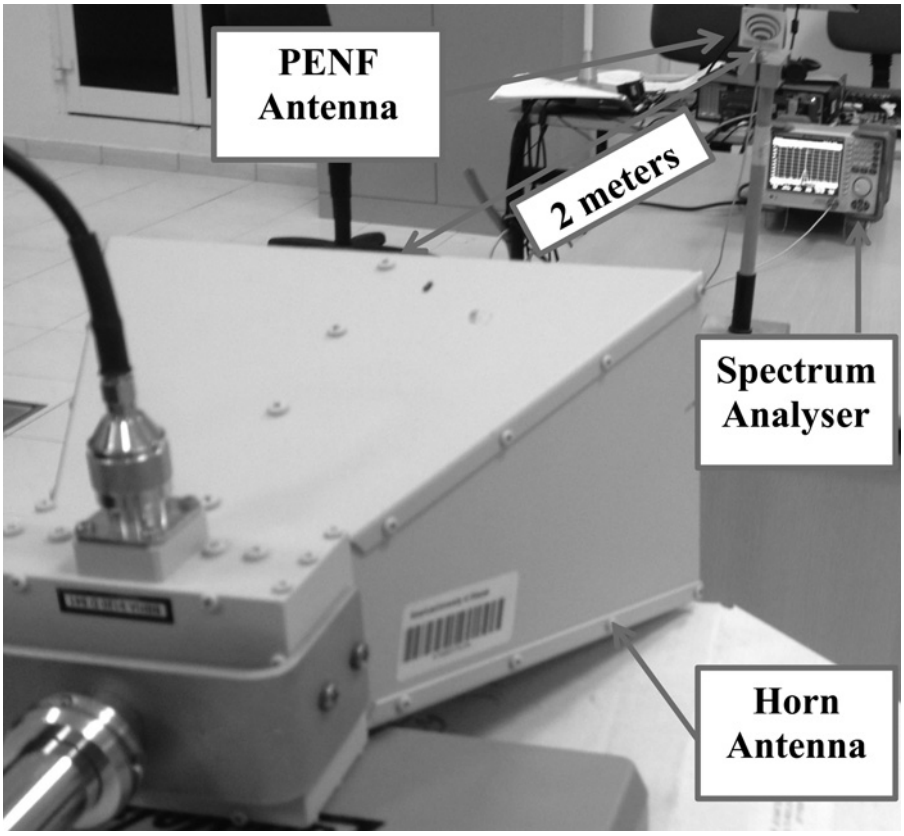

Fig. 10 *Gain measurement setup (AUT)*

Table 3 Simulated against measured gain of PENF antenna on FR4 substrate

Frequency, GHz	Simulated gain, dBi	Measured gain, dBi
1	−4.6	−8.4
1.92	0.5	0.74
2.05	1.24	1.4
2.7	0.58	1.6

measurement, VNA was calibrated using the calibration kit (Agilent 85033E) shown in the figure. Since only $S11$ measurement is required, only one of VNA ports was calibrated.

In Fig. 9, a comparison of the antenna's simulated return loss response in ADS (blue) against the practical measurement (black) is shown. The results in the figure agree well for the two deep notches observed at 1.6 and 1.9 GHz (GMS 1800). The simulation is showing an additional notch at 2.7 GHz which is not achieved in practical measurements. The fabrication tolerance could be considered as the reason for the mismatch seen at higher frequencies. Overall, the simulation and practical responses are following the same trend confirming the multiband nature of the PENF antenna structure.

The practical setup to measure the gain of the PENF antenna on FR4 substrate is shown in Fig. 10. This setup consists of an RF signal synthesiser (1–3 GHz), a standard gain horn antenna as a transmitting element, the PENF antenna as a receiving element and a VNA spectrum analyser (DC – 6 GHz) to measure the received signal power. At each frequency, the generated signal was transmitted by the horn antenna which was placed at a distance of 2 m away from the PENF antenna in order to operate in the far-field region. The gain of the PENF antenna at each frequency was obtained. Table 3 presents the simulated and measured gains of the PENF antenna fabricated on FR4 substrate.

The radiation pattern of the PENF antenna on FR4 substrate was obtained using Lab-Volt (LVDAM-ANT) antenna measurement system. The *E*-plane, *H*-plane and cross-polarisation patterns of the PENF antenna were measured at the proposed frequencies of operations: 1.53, 1.92, 2.05 and 2.7 GHz. The selected frequencies were chosen based on the return loss response of the antenna to target GSM 1800 and WLAN bands. Figs. 11*a*–*d* show the obtained measurement results. Although the pattern at 1.92 GHz has two nulls, the overall patterns at this frequency and other frequencies are nearly omni-directional. The *E*-plane cross-polarisation components of the radiation pattern verify that the polarisation of the PENF antenna is not purely linear and the antenna is capable of receiving the signal when the transmitter is positioned vertically relative to the PENF antenna. Additionally, the *E*-plane and the *H*-plane patterns of the PENF antenna at all frequencies of interest are shown in Figs. 12*a* and *b*, respectively.

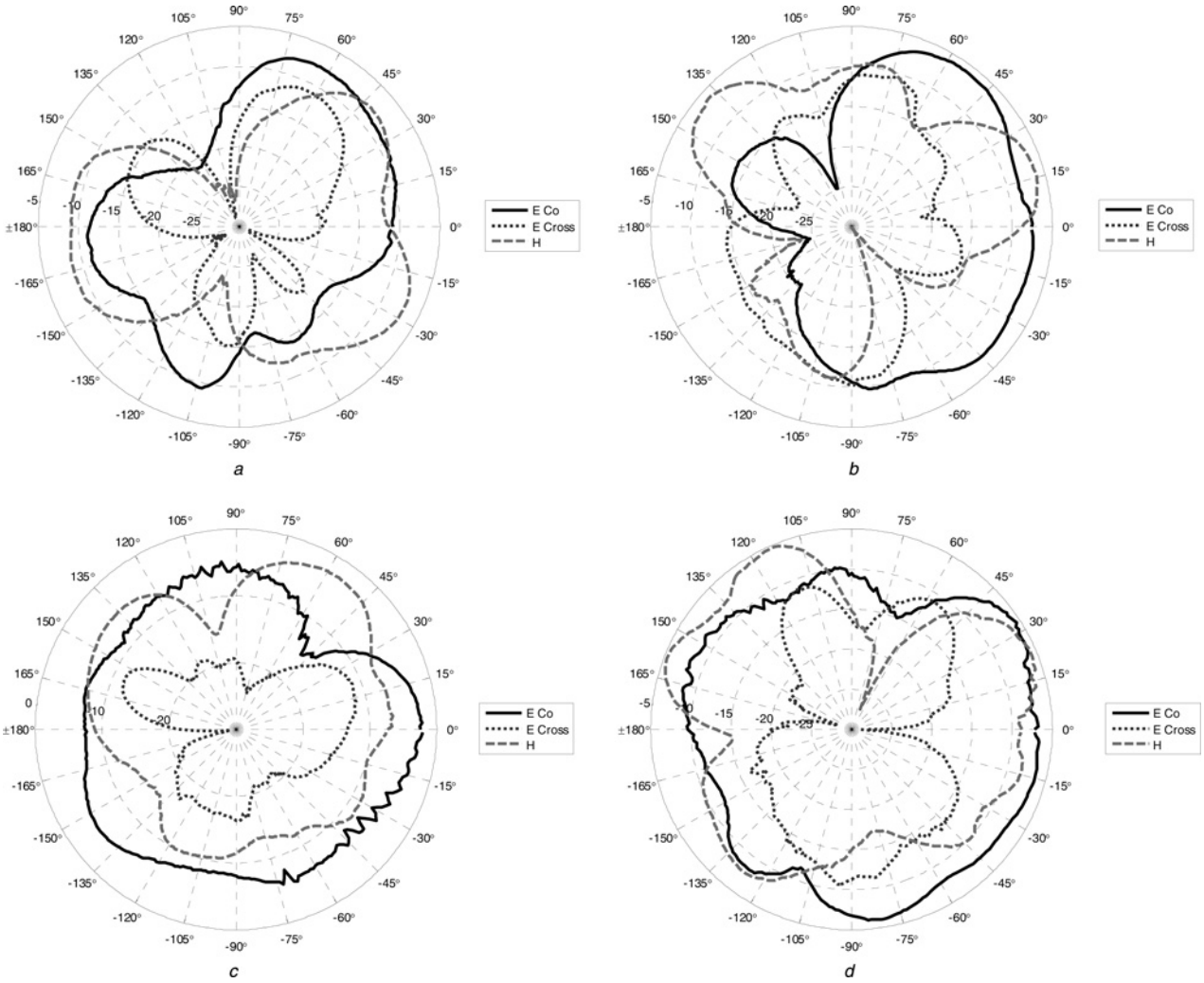

Fig. 11 *Measured far-field radiation patterns of PENF antenna on FR4 substrate at*

a 1.53 GHz
b 1.92 GHz
c 2.05 GHz
d 2.7 GHz

IET Microw. Antennas Propag., 2015, Vol. 9, Iss. 10, pp. 1045–1053

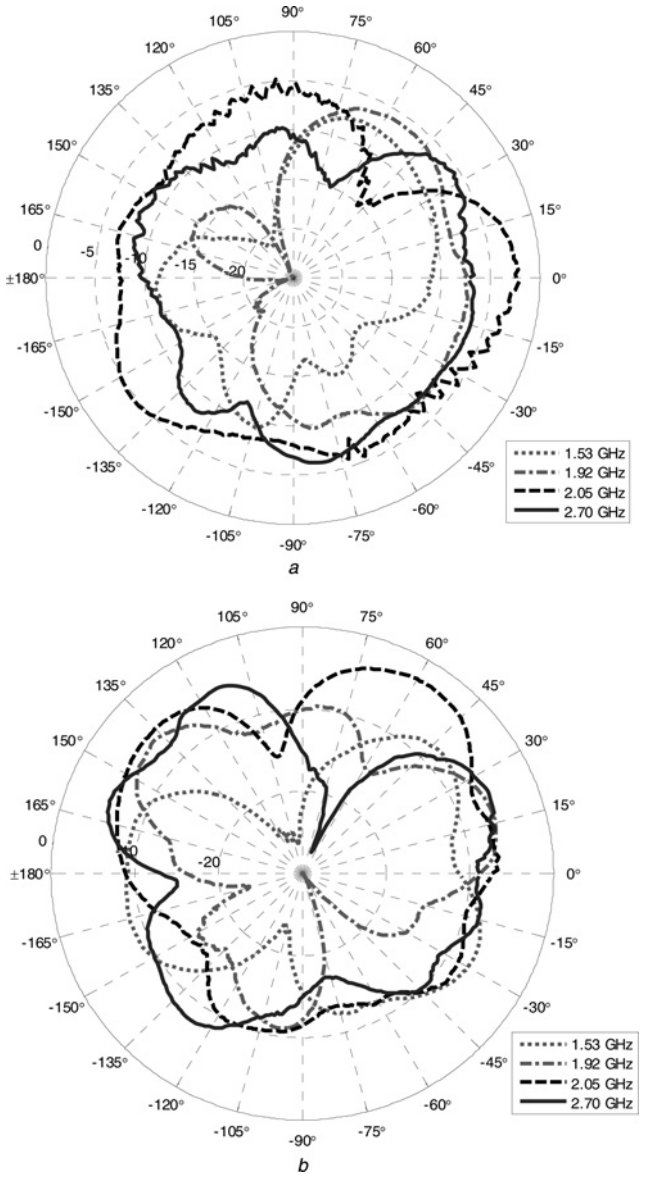

Fig. 12 *Measured far-field radiation pattern of PENF antenna on FR4 substrate at all frequencies of operation*

a E-plane
b H-plane

Overall, the obtained patterns verify that the PENF antenna closely mimics the omni-directional antenna radiation pattern. Consequently, the designed antenna is suitable for EM energy harvesting applications where the incident signals are unknown.

5 Conclusions

In this paper, the design of a novel PENF multiband antenna is presented. The PENF antenna is simple, compact and easy to be integrated with other electronic circuitry. The PENF antenna, fed by a 50 Ω microstrip line, consists of nested elliptical geometries on two conductor layers of substrate. Hilbert fractal structures are added to the sides of the feed line to improve the impedance matching along the desired frequencies. Simulation results of PENF antenna on Rogers 6010 laminate show excellent reflection and omni-directional radiation properties at the design frequency bands. The proposed antenna covers GSM 900, 2.4 GHz Bluetooth/WLAN, 3.2 GHz (Radiolocation, 3G), 3.8 GHz (for LTE, 4G) and 5 GHz Wi-Fi bands and is intended to be used in EM energy harvesting applications. The proposed structure is also designed and fabricated using FR4 substrate. Measurement and simulation results of return loss and gain of the fabricated PENF antenna closely match. The measured radiation patterns of PENF antenna in different planes verify the omni-directional feature of the proposed antenna. This feature is of interest in EM energy harvesting applications to receive the ambient signals from all directions. The PENF antenna structure is being used as part of the harvester system developed in this research.

6 Acknowledgments

The authors are grateful to Mubadala Technologies and to the Semiconductor Research Corporation (SRC) for their technical support and financial grant of this work.

7 References

1 Kang, C.C., Olokede, S.S., Mahyuddin, N.M., Ain, M.F.: 'Radio frequency energy harvesting using circular spiral inductor antenna'. 2014 IEEE 15th Annual Wireless and Microwave Technology Conf. (WAMICON), 6–6 June 2014, pp. 1–5
2 Xi, S., Bo, L., Shahshahan, N., Goldsman, N., Salter, T.S., Metze, G.M.: 'A planar dual-band antenna design for RF energy harvesting applications'. 2011 Int. Semiconductor Device Research Symp. (ISDRS), 7–9 December 2011, pp. 1–2.
3 Tavares, J., Barreca, N., Saraiva, H.M., *et al.*: 'Spectrum opportunities for electromagnetic energy harvesting from 350 MHz to 3 GHz'. 2013 Seventh Int. Symp. on Medical Information and Communication Technology (ISMICT), 6–8 March 2013, pp. 126–130
4 Nimo, A., Grgic, D., Reindl, L.M.: 'Ambient electromagnetic wireless energy harvesting using multiband planar antenna'. 2012 Ninth Int. Multi-Conf. on Systems, Signals and Devices (SSD), 20–23 March 2012, pp. 1–6
5 Rafaei Booket, M., Jafargholi, A., Kamyab, M., Eskandari, H., Veysi, M., Mousavi, S.M.: 'Compact multi-band printed dipole antenna loaded with single-cell metamaterial', *IET Microw. Antennas Propag.*, 2012, **6**, (1), pp. 17–23
6 Ali, M.M.M., Azmy, A.M., Haraz, O.M.: 'Design and implementation of reconfigurable quad-band microstrip antenna for MIMO wireless communication applications'. 2014 31st National Radio Science Conf. (NRSC), 28–30 April 2014, pp. 27–34
7 Ansal, K.A., Shanmuganantham, T.: 'Compact novel ACS fed antenna with defected ground for triple frequency operation'. 2013 Annual Int. Conf. on Emerging Research Areas and 2013 Int. Conf. on Microelectronics, Communications and Renewable Energy (AICERA/ICMiCR), 4–6 June 2013, pp. 1–4
8 Ma, C., Kuai, Z., Xiao-Wei, Z., Wen-Jia, Z.: 'A broadside-coupled feeding planar multiband antenna'. 2013 IEEE Antennas and Propagation Society Int. Symp. (APSURSI), 7–13 July 2013, pp. 520–521
9 Pinuela, M., Mitcheson, P.D., Lucyszyn, S.: 'Ambient RF energy harvesting in urban and semi-urban environments', *IEEE Trans. Microw. Theory Tech.*, 2013, **61**, (7), pp. 2715–2726
10 Lim, T.B., Lee, N.M., Poh, B.K.: 'Feasibility study on ambient RF energy harvesting for wireless sensor network'. 2013 IEEE MTT-S Int. Microwave Workshop Series on RF and Wireless Technologies for Biomedical and Healthcare Applications (IMWS-BIO), 9–11 December 2013, pp. 1–3
11 Pozar, D.M.: 'Microwave engineering' (John Wiley & Sons, Crawfordsville, USA, 1998, 2nd edn.)
12 Surabhi, D., Vivekanand, M., Kosta, Y.P.: 'Metamaterial inspired patch antenna miniaturization technique for Satellite'. 2012 First Int. Conf. on Emerging Technology Trends in Electronics, Communication and Networking (ET2ECN), 19–21 December 2012, pp. 1–6
13 Ray, K.P.: 'Design aspects of printed monopole antennas for ultra-wide band applications', *Int. J. Antennas Propag.*, 2008, **2008**, pp. 8, Article ID 713858
14 Bras, L., Carvalho, N.B., Pinho, P.: 'Circular polarized planar elliptical antenna array'. 2013 Seventh European Conf. on Antennas and Propagation (EuCAP), 8–12 April 2013, pp. 891–893
15 Venkatesulu, S., Varadarajan, S., Giriprasad, M.N., Thenappan, S.: 'Printed elliptical planar monopole patch antenna for wireless communications'. 2013 Int. Conf. on Green Computing, Communication and Conservation of Energy (ICGCE), 12–14 December 2013, pp. 314–319
16 Sayidmarie, K.H., Fadhel, Y.A.: 'Design aspects of UWB printed elliptical monopole antenna with impedance matching'. 2012 Loughborough Antennas and Propagation Conf. (LAPC), 12–13 November 2012, pp. 1–4
17 Vinoy, K.J., Jose, K.A., Varadan, V.K., Varadan, V.V.: 'Resonant frequency of Hilbert curve fractal antennas'. 2001, IEEE Antennas and Propagation Society Int. Symp., 8–13 July 2001, vol. 3, pp. 648–651
18 Prombutr, N., Akkaraaektharm, P.: 'Analysis and design of Hilbert curve fractal antenna feed with coplanar wave guide for multiband wireless communications', *Int. J. Eng.*, 2008, **2**, (3), pp. 1–11
19 Kumar, N., Sinha, M.K., Bandyopadhyay, L.K., Kumar, S.: 'Design of a wideband reduced size microstrip antenna in VHF/lower UHF range'. URSI Proc., New Delhi, October 2005
20 Gupta, N.: 'Material selection of LTCC based microstrip patch antenna substrate using Ashby's approach'. 2014 Int. Symp. on Computer, Consumer and Control (IS3C), 10–12 June 2014, pp. 1018–1021
21 Balanis, C.A.: 'Antenna theory: analysis and design' (John Wiley and Sons, Hoboken, NJ, USA, 2005, 3rd edn.)